J. Fluid Mech. (2007), *vol.* 577, *pp.* 287–307.
doi:10.1017/S0022112006003260 Printed in the United Kingdom

Two-point similarity in temporally evolving plane wakes

D. EWING[1]†, W. K. GEORGE[2], M. M. ROGERS[3] AND R. D. MOSER[4]

[1]Department of Mechanical Engineering, McMaster University, Hamilton, ON, Canada
[2]Department of Applied Mechanics, Chalmers University of Technology, Gothenburg, Sweden
[3]NASA Ames Research Center, Moffett Field, CA, USA
[4]Department of Mechanical Engineering and Institute for Computational Engineering and Sciences, University of Texas at Austin, 1 University Station, Stop C22, Austin, TX, USA

(Received 7 December 2004 and in revised form 12 June 2006)

The governing equations for the two-point correlations of the turbulent fluctuating velocity in the temporally evolving wake were analysed to determine whether they could have equilibrium similarity solutions. It was found that these equations could have such solutions for a finite-Reynolds-number wake, where the two-point velocity correlations could be written as a product of a time-dependent scale and a function dependent only on similarity variables. It is therefore possible to collapse the two-point measures of all the scales of motions in the temporally evolving wake using a single set of similarity variables. As in an earlier single-point analysis, it was found that the governing equations for the equilibrium similarity solutions could not be reduced to a form that was independent of a growth-rate dependent parameter. Thus, there is not a single 'universal' solution that describes the state of the large-scale structures, so that the large-scale structures in the far field may depend on how the flow is generated.

The predictions of the similarity analysis were compared to the data from two direct numerical simulations of the temporally evolving wakes examined previously. It was found that the two-point velocity spectra of these temporally evolving wakes collapsed reasonably well over the entire range of scales when they were scaled in the manner deduced from the equilibrium similarity analysis. Thus, actual flows do seem to evolve in a manner consistent with the equilibrium similarity solutions.

1. Introduction

A widely accepted idea about turbulent flows is that most turbulent free shear flows eventually evolve to a state in which the profiles of the mean velocity and Reynolds stresses are self-similar (e.g. Wygnanski, Champagne & Marasli 1986; Hussein, Capp & George 1994). There has been considerable disagreement, though, as to whether there is a unique or 'universal' self-similar solution that describes the far field of each type of flow. This idea of a universal self-similar solution for each type of flow was proposed early in the investigation of turbulent shear flows (cf.

† Current address: Department of Mechanical and Materials Engineering, Queen's University, Kingston, Canada K7L 3N6.

Townsend 1956) and has been widely accepted since (e.g. Tennekes & Lumley 1972; Narasimha 1992; Pope 2000; Durbin & Reif 2001). George (1989, 1995) showed that there was a family of similarity solutions for the governing equations in each type of free-shear flow that includes a parameter that depends on the growth rate of the flow. George argued that the development of the flows into the far field could depend on the initial or source conditions of the flows and, indeed, Wygnanski *et al.* (1986) and a number of more recent investigations (e.g. Ghosal & Rogers 1997; Moser, Rogers & Ewing 1998; Slessor, Bond & Dimotakis 1998; Mi, Nobes & Nathan 2001; Johansson, George & Gourlay 2003) have found that the development of jets, wakes, or shear layers generated by different sources do seem to develop to different states.

Townsend (1956) noted the possibility that turbulent flows could have non-unique self-similar solutions, but conjectured that the large-scale structures generated in the near field would break down and the new large-scale structures would approach a universal state that depended only on the type of shear flow. Thus, Townsend recognized that the 'equilibrium' observed in the single-point moments was a measure of an 'equilibrium' in the processes that govern the development of the underlying structures, which are not well characterized by the single-point moments. Therefore it is useful to examine two-point measures of the turbulence to determine if the underlying structures in the flow are evolving in an equilibrium manner, and whether there is more than a single universal solution for these measures in each family of flows.

Since Townsend (1956), there has been considerable interest in characterizing the development of the large-scale structures in turbulent shear flows. Of particular interest have been the large-scale structures that occur in the plane wake. One of the earliest investigations of these structures was conducted by Grant (1958), who reported measurements of the two-point and two-time correlations of the fluctuating velocity field in the wake and used these measurements to revise Townsend's 'double-roller eddy' model for the structures occurring across the wake (and also the boundary layer). Keffer (1965) conjectured that the double-roller eddies observed in wakes were horseshoe vortices formed from an instability in the spanwise roller vortices. Later investigations found that the roller eddies did appear to be horseshoe vortices caused by an instability in the spanwise shear layer (e.g. Antonia *et al.* 1987; Hayakawa & Hussain 1989, and references therein) though there was some evidence of single roller eddies (e.g. Townsend 1979; Mumford 1983) or rib structures in the wake (e.g. Hayakawa & Hussain 1989). Antonia *et al.* (1987) also noted that the structures in the far field were similar to those observed in the near field, but occurred further from the wake centreline. Grant (1958) had found that lateral correlations measured 500 and 1000 diameters downstream of a cylinder collapsed when they were scaled by the appropriate similarity variables, but this does not appear to have been re-examined in later investigations.

There is evidence that the large-scale structures present in the far field of wakes depend on the wake source. For example, Bonnet, Delville & Garem (1986) found that the two-point velocity correlations measured in the wake behind a flat plate with turbulent boundary layers were significantly different from those reported by Grant for the wake produced by a circular cylinder, particularly in the lateral direction. Bonnet *et al.* suggested that the transition of the wake behind a body with laminar boundary layers could create different structures from those formed when two independent turbulent boundary layers meet behind a body (as was the case in their flow). Indeed, Weygandt & Mehta (1993) found that the structures in the far-field wake of a plate with turbulent boundary layers were more three-dimensional than those in the

far-field wake of a plate with laminar boundary layers. Moser *et al.* (1998) also found that differences in the large-scale structures initially present in direct numerical simulations of temporally evolving wakes did seem to persist into the far field of these flows. Not surprisingly, investigations have shown that the structures formed during the transition process in plane wakes depend on the initial conditions (e.g. Williamson & Prasas 1993; Maekawa, Mansour & Buell 1992) and that the initial development of the structures may be more complex than suggested by phase-averaged measurements (Brede, Leder & Westergaard 2003).

Heretofore, there have been only a few attempts to analyse the equations for the two-point velocity correlations in turbulent flows in order to examine whether they have self-similar solutions. These investigations have primarily focused on homogeneous flows, including decaying isotropic turbulence (e.g. von Kármán & Howarth 1938; Batchelor 1948; George 1992; Speziale & Bernard 1992), or homogeneous shear flow (George & Gibson 1992). Ewing & George (1995) demonstrated that the governing equations for the two-point velocity correlation in the spatially developing jet have self-similar solutions. Experimental investigations of the two-point measures on different downstream planes in spatially evolving flows include studies of the plane jet by Gordeyev & Thomas (2000), the round jet by Gamard, Jung & George (2004), and the axisymmetric wake by Johansson & George (2006). All found that the results seem to exhibit two-point similarity as predicted by Ewing (1995), although none considered the correlations in the streamwise direction.

The present work considers the change in the two-point correlations at long times in the temporally evolving wake. This work follows the investigation by Moser *et al.* (1998) that examined the similarity of the single-point moments in temporally evolving plane wakes with different initial conditions. Here, the governing equations for the two-point velocity correlations are analysed to determine whether these equations have equilibrium similarity solutions. The data from two direct numerical simulations of the temporally evolving wake considered by Moser *et al.* are then used to determine whether the derived equilibrium similarity solutions do describe the evolution of the different scales of motion in these simulations. Finally, some implications of these self-similar solutions on different measures of the turbulent structures are presented.

2. Analysis of the governing equations

The objective here is to determine whether the governing equations for the two-point velocity correlation tensor can have equilibrium similarity solutions for a temporally evolving plane wake. The temporally evolving wake is homogeneous in the mean flow and lateral directions and spreads in the inhomogeneous direction over time. The governing equations for the two-point single-time correlations of the fluctuating velocity (cf. Hinze 1975) in this flow reduce to

$$\begin{aligned}
&\frac{\partial \overline{u_i u'_j}}{\partial t} + (U_1 - U'_1)\frac{\partial \overline{u_i u'_j}}{\partial r_1} \\
&\quad = -\frac{1}{\rho}\left[\frac{\partial}{\partial r_1}(\overline{pu'_j}\delta_{i1} - \overline{p'u_i}\delta_{j1}) + \frac{\partial \overline{pu'_j}}{\partial x_2}\delta_{i2} + \frac{\partial \overline{p'u_i}}{\partial x'_2}\delta_{j2} + \frac{\partial}{\partial r_3}(\overline{pu'_j}\delta_{i3} - \overline{p'u_i}\delta_{j3})\right] \\
&\qquad - \frac{\partial}{\partial r_1}(\overline{u_1 u_i u'_j} - \overline{u'_1 u_i u'_j}) - \frac{\partial \overline{u_2 u_i u'_j}}{\partial x_2} - \frac{\partial \overline{u'_2 u_i u'_j}}{\partial x'_2} - \frac{\partial}{\partial r_3}(\overline{u_3 u_i u'_j} - \overline{u'_3 u_i u'_j}) \\
&\qquad - \overline{u'_j u_2}\frac{\partial U_1}{\partial x_2}\delta_{i1} - \overline{u_i u'_2}\frac{\partial U'_1}{\partial x'_2}\delta_{j1} + \nu\left(2\frac{\partial^2}{\partial r_1^2} + \frac{\partial^2}{\partial x_2^2} + \frac{\partial^2}{\partial x_2'^2} + 2\frac{\partial^2}{\partial r_3^2}\right)\overline{u_i u'_j}, \qquad (2.1)
\end{aligned}$$

where the unprimed variables are evaluated at one point in the wake, x_α, and the primed variables are evaluated at a second arbitrary point in the wake, x'_α, at the same time. Here, $r_1 = x_1 - x'_1$ and $r_3 = x_3 - x'_3$ are the separation distances in the homogeneous streamwise and lateral directions of the wake, respectively.

It is proposed that the two-point correlations in (2.1) have solutions of the form

$$\overline{u_i(x_1, x_2, x_3, t)u'_j(x'_1, x'_2, x'_3, t)} = Q^{i,j}_s(t)q_{i,j}(\zeta, \eta, \eta', \xi, Re, *), \tag{2.2}$$

$$\overline{pu'_j} = \Pi^{,j}_{s,1}(t)\pi^1_{,j}(\zeta, \eta, \eta', \xi, Re, *), \tag{2.3}$$

$$\overline{p'u_i} = \Pi^{i,}_{s,2}(t)\pi^2_{i,}(\zeta, \eta, \eta', \xi, Re, *), \tag{2.4}$$

$$\overline{u_k u_i u'_j} = T^{ki,j}_{s,1}(t)tt^1_{ki,j}(\zeta, \eta, \eta', \xi, Re, *), \tag{2.5}$$

and

$$\overline{u_i u'_k u'_j} = T^{i,kj}_{s,2}(t)tt^2_{i,kj}(\zeta, \eta, \eta', \xi, Re, *), \tag{2.6}$$

where

$$\zeta = r_1/\delta_1(t), \tag{2.7}$$

$$\eta = x_2/\delta(t), \tag{2.8}$$

$$\eta' = x'_2/\delta(t), \tag{2.9}$$

and

$$\xi = r_3/\delta_3(t) \tag{2.10}$$

are the similarity coordinates. Thus, the two-point correlations here are written as the product of a time-dependent scale and a solution that depends only on similarity variables. The superscripts in these relationships are not indices so they should not be considered when applying the summation convention. The subscripts are indices so the summation convention applies to repeated subscripts in the following equations. The length scales in the x_1- and x_3-directions, δ_1 and δ_3, are arbitrary at this point and will be determined from the constraints imposed by the governing equations. The symbol $*$ has been included in the solutions to allow for any dependence on the source conditions of the flow.

The averaged momentum equations include information about the development of the flow that is not included in the transport equations for either the single-point turbulence Reynolds stresses or the two-point velocity correlations. Thus, the results from the analysis of these equations must be considered in the analysis of either the single-point or the two-point equations. Moser *et al.* (1998) showed that the mean momentum equations have equilibrium similarity solutions of the form

$$\Delta U_1 = U_\infty - U_1(x_2, t) = U_s(t)f(\eta) \tag{2.11}$$

and

$$\overline{u_1 u_2} = R_s(t)g(\eta), \tag{2.12}$$

only when

$$U_s(t) \propto \frac{1}{\delta(t)} \tag{2.13}$$

and

$$R_s(t) \propto U_s(t)\frac{\mathrm{d}\delta}{\mathrm{d}t}. \tag{2.14}$$

Substituting the proposed similarity solutions into the governing equations yields

$$\left[\frac{\mathrm{d}Q_s^{i,j}}{\mathrm{d}t}\right] q_{i,j} - \left[\frac{Q_s^{i,j}}{\delta_1}\frac{\mathrm{d}\delta_1}{\mathrm{d}t}\right]\zeta\frac{\partial q_{i,j}}{\partial\zeta} - \left[\frac{Q_s^{i,j}}{\delta}\frac{\mathrm{d}\delta}{\mathrm{d}t}\right]\left(\eta\frac{\partial}{\partial\eta}+\eta'\frac{\partial}{\partial\eta'}\right) q_{i,j} - \left[\frac{Q_s^{i,j}}{\delta_3}\frac{\mathrm{d}\delta_3}{\mathrm{d}t}\right]\xi\frac{\partial q_{i,j}}{\partial\xi}$$
$$+\left[\frac{U_s(t)Q_s^{i,j}}{\delta_1}\right]\{f(\eta')-f(\eta)\}\frac{\partial q_{i,j}}{\partial\zeta} = -\frac{1}{\rho}\left(\left[\frac{\Pi_{s,1}^{,j}}{\delta_1}\right]\frac{\partial\pi_{,j}^1}{\partial\zeta}\delta_{i1} - \left[\frac{\Pi_{s,2}^{i,}}{\delta_1}\right]\frac{\partial\pi_{i,}^2}{\partial\zeta}\delta_{j1}\right.$$
$$\left.+\left[\frac{\Pi_{s,1}^{,j}}{\delta}\right]\frac{\partial\pi_{,j}^1}{\partial\eta}\delta_{i2} + \left[\frac{\Pi_{s,2}^{i,}}{\delta}\right]\frac{\partial\pi_{i,}^2}{\partial\eta'}\delta_{j2} + \left[\frac{\Pi_{s,1}^{,j}}{\delta_3}\right]\frac{\partial\pi_{,j}^1}{\partial\xi}\delta_{i3} - \left[\frac{\Pi_{s,2}^{i,}}{\delta_3}\right]\frac{\partial\pi_{i,}^2}{\partial\xi}\delta_{j3}\right)$$
$$-\left[\frac{T_{s,1}^{1i,j}}{\delta_1}\right]\frac{\partial tt_{1i,j}^1}{\partial\zeta} + \left[\frac{T_{s,2}^{i,1j}}{\delta_1}\right]\frac{\partial tt_{i,1j}^2}{\partial\zeta} - \left[\frac{T_{s,2}^{2i,j}}{\delta}\right]\frac{\partial tt_{2i,j}^2}{\partial\eta} - \left[\frac{T_{s,2}^{i,2j}}{\delta}\right]\frac{\partial tt_{i,2j}^2}{\partial\eta'}$$
$$-\left[\frac{T_{s,1}^{3i,j}}{\delta_3}\right]\frac{\partial tt_{3i,j}^1}{\partial\xi} + \left[\frac{T_{s,2}^{i,3j}}{\delta_3}\right]\frac{\partial tt_{i,3j}^2}{\partial\xi} + \left[\frac{Q_s^{2,j}U_s}{\delta}\right]q_{2,j}\frac{\mathrm{d}f}{\mathrm{d}\eta}\delta_{i1} + \left[\frac{Q_s^{i,2}U_s}{\delta}\right]q_{i,2}\frac{\mathrm{d}f}{\mathrm{d}\eta'}\delta_{j1}$$
$$+\nu\left(2\left[\frac{Q_s^{i,j}}{\delta_1^2}\right]\frac{\partial^2}{\partial\zeta^2} + \left[\frac{Q_s^{i,j}}{\delta^2}\right]\frac{\partial^2}{\partial\eta^2} + \left[\frac{Q_s^{i,j}}{\delta^2}\right]\frac{\partial^2}{\partial\eta'^2} + 2\left[\frac{Q_s^{i,j}}{\delta_3^2}\right]\frac{\partial^2}{\partial\xi^2}\right) q_{i,j}. \tag{2.15}$$

If all the terms in the equations are first-order, the equations can have equilibrium similarity solutions only if the time-dependent portion of each term (in square brackets) is proportional. Physically, this would imply that the production and dissipation of energy at the different scales of motion, and the transfer of energy between the different scales of motion, are in equilibrium as the flow evolves.

Constraints for δ_1 and δ_3 can be determined by considering the nonlinear energy transfer terms in the equations. In particular, the time-dependent portions of the energy transfer terms in the equation for $\overline{u_1u_1'}$ and the equation for $\overline{u_2u_1'}$ are only proportional if

$$\left[\frac{\Pi_{s,1}^{,1}}{\delta_1}\right] \propto \left[\frac{T_{s,1}^{21,1}}{\delta}\right] \tag{2.16}$$

and

$$\left[\frac{\Pi_{s,1}^{,1}}{\delta}\right] \propto \left[\frac{T_{s,1}^{12,1}}{\delta_1}\right], \tag{2.17}$$

respectively. The scales for $T_{s,1}^{21,1}$ and $T_{s,2}^{12,1}$ must be equal since $\overline{u_2u_1u_1'} = \overline{u_1u_2u_1'}$. Thus, it follows that $\delta_1^2 \propto \delta^2$ or $\delta_1 \propto \delta$. A similar approach can be applied to the energy transfer terms in the equations for $\overline{u_3u_3'}$ and $\overline{u_3u_2'}$ to show that $\delta_3 \propto \delta$. Thus, the characteristic length scales of the turbulent motions grow at the same rate in all directions as the flow evolves.

The time-dependent scales for $\overline{u_1u_2'}$ and $\overline{u_2u_1'}$ must be consistent with the scale for $\overline{u_1u_2}$ from the momentum equation in the limit of zero separation. Thus,

$$Q_s^{1,2}(t) = Q_s^{2,1}(t) \propto R_s(t) \propto U_s(t)\frac{\mathrm{d}\delta}{\mathrm{d}t}. \tag{2.18}$$

Using (2.18) and comparing the scales for the production and convection terms in the $\overline{u_1u_1'}$ equation yields

$$Q_s^{1,1} \propto U_s^2. \tag{2.19}$$

The scales for $\overline{u_2u_2'}$ and $\overline{u_3u_3'}$ are deduced by recognizing that in an incompressible flow

$$\frac{\partial \overline{pu_j'}}{\partial x_j'} = 0. \tag{2.20}$$

Substituting the similarity solutions into this equation yields

$$-\left[\frac{\Pi_{s,1}^{,1}}{\delta_1}\right]\frac{\partial \pi_{,1}^1}{\partial \zeta} + \left[\frac{\Pi_{s,1}^{,2}}{\delta}\right]\frac{\partial \pi_{,2}^1}{\partial \eta'} - \left[\frac{\Pi_{s,1}^{,3}}{\delta_3}\right]\frac{\partial \pi_{,3}^1}{\partial \xi} = 0. \tag{2.21}$$

The proposed similarity solutions are again consistent with this equation only if the time-dependent terms (in square brackets) are proportional. Using this constraint, and comparing the convection and pressure transfer terms in the $\overline{u_\alpha u_\alpha'}$ equations implies that

$$Q_s^{1,1} \propto Q_s^{2,2} \propto Q_s^{3,3} \propto U_s^2. \tag{2.22}$$

The remaining terms in (2.15) are proportional only if

$$Q_s^{1,3} \propto Q_s^{3,1} \propto Q_s^{2,3} \propto Q_s^{3,2} \propto U_s^2(t), \tag{2.23}$$

$$\Pi_{s,1}^{,j} \propto \Pi_{s,2}^{i,} \propto U_s^3, \tag{2.24}$$

and

$$T_{s,1}^{ki,j} \propto T_{s,2}^{i,kj} \propto Q_s^{i,j}\frac{\mathrm{d}\delta}{\mathrm{d}t}. \tag{2.25}$$

The constants of proportionality in these relationships may depend on the source conditions of the flow.

The growth rate of the similarity length scale can be deduced by comparing the scales for the unsteady term and the production term in the $\overline{u_1u_2'}$ equation; i.e.

$$\left[\frac{Q_s^{1,2}}{\delta}\frac{\mathrm{d}\delta}{\mathrm{d}t}\right] \propto \left[\frac{U_s Q_s^{2,2}}{\delta}\right] \rightarrow \left(\frac{1}{U_s}\frac{\mathrm{d}\delta}{\mathrm{d}t}\right)^2 = \beta^2 \rightarrow \delta = \beta(t - t_o)^{1/2}, \tag{2.26}$$

since $U_s \propto 1/\delta$ from the mean momentum equation. Finally, the convection and viscous terms in the equations can be proportional only if

$$\left[\frac{U_s Q_s^{i,j}}{\delta}\right] \propto \left[\nu\frac{Q_s^{i,j}}{\delta^2}\right] \rightarrow Re_\delta = \frac{U_s\delta}{\nu} = \text{const.} \tag{2.27}$$

This is the same constraint deduced from the integrated mean momentum equation, so the viscous terms can be retained in the governing equations for the two-point velocity correlations without imposing any additional constraints in this constant-Reynolds-number flow. Thus, the governing equations for the two-point velocity correlations indeed admit equilibrium similarity solutions that describe the evolution of all the scales of motion for turbulent wakes with finite Reynolds numbers. It is straightforward to show that the *more general* similarity solutions deduced here for the two-point correlations reduce to forms consistent with the *more restricted* solutions for the single-point moments in the limit of zero separation distance.

The functional form of these solutions does depend on the Reynolds numbers of the wake, so different scaling should still be used when comparing measures of the large- and small-scale motions from wakes with different Reynolds numbers. Further, as with the single-point equations (cf. Moser *et al.* 1998), there was not a unique choice for the time-dependent scales of the two-point correlations that would allow

the growth-rate-dependent parameter β to be removed from the governing equations for the similarity solutions. Therefore, there is a family of equilibrium similarity solutions for the governing equations of the two-point velocity correlation tensor in the wake, and thus, the large-scale structures present in the self-similar wake may depend on the source conditions used to generate the flow.

2.1. *Implications for the spectra and the proper orthogonal decomposition (POD)*

The existence of the equilibrium similarity solutions for the two-point velocity correlations has implications on how the energy is distributed amongst the different scales of motion in the flow, and thus on the representation of this energy distribution. For example, when the two-point velocity correlations have equilibrium solutions, it follows immediately that one-dimensional spectra in the x_1-direction given by

$$F_{ij}^1(k_1, x_2, x_2', r_3) = \frac{1}{2\pi}\int_{-\infty}^{\infty} R_{i,j}(r_1, x_2, x_2', r_3)\exp(-\mathrm{i}k_1 r_1)\,\mathrm{d}r_1 \tag{2.28}$$

can be written as

$$\begin{aligned} F_{ij}^1(k_1, x_2, x_2', r_3) &= \frac{1}{2\pi}\left[Q_s^{i,j}\delta\right]\int_{-\infty}^{\infty} q_{i,j}(\zeta, \eta, \eta', \xi)\exp(-\mathrm{i}\tilde{k}_1\zeta)\,\mathrm{d}\zeta, \\ &= \left[Q_s^{i,j}\delta\right]\tilde{F}_{ij}^1(\tilde{k}_1, \eta, \eta', \xi), \end{aligned} \tag{2.29}$$

where k_1 and $\tilde{k}_1 = k_1\delta$ are the dimensional and similarity wavenumbers, respectively, in the x_1-direction. It also follows that the one-dimensional spectra in the x_3-direction can be written as

$$F_{ij}^3(r_1, x_2, x_2', k_3) = \left[Q_s^{i,j}\delta\right]\tilde{F}_{ij}^3(\zeta, \eta, \eta', \tilde{k}_3), \tag{2.30}$$

where k_3 and $\tilde{k}_3 = k_3\delta$ are the physical and similarity wavenumbers in the x_3-direction.

The same can be shown for the representation of the different motions in the inhomogeneous direction using the proper orthogonal decomposition (POD). In the POD, the turbulent motions are represented by orthogonal functions that are solutions to the integral eigenvalue problem given by (Lumley 1970)

$$\int_{-\infty}^{\infty} R_{i,j}(x_2, x_2')\phi_j^n(x_2')\,\mathrm{d}x_2' = \Lambda_n\phi_i^n(x_2), \tag{2.31}$$

where the functions are defined to be orthonormal; i.e.

$$\int_{-\infty}^{\infty} \phi_j^n(x_2')\phi_j^{m*}(x_2')\,\mathrm{d}x_2' = \delta_{mn}. \tag{2.32}$$

Here, $*$ denotes the complex conjugate. (The separations in the x_1- and x_3-directions have been set to zero in these equations for simplicity, but these separation distances could easily have been included or the POD could easily have been applied after the two-point velocity correlation had been Fourier transformed in these directions.)

When the two-point velocity correlations have similarity solutions, these equations can be written as

$$\left[\frac{Q_s^{i,j}}{U_s^2}\right]\int_{-\infty}^{\infty} q_{i,j}(\eta, \eta')\chi_j^n(\eta')\,\mathrm{d}\eta' = \tilde{\Lambda}_n\chi_i^n(\eta), \tag{2.33}$$

and

$$\int_{-\infty}^{\infty} \chi_j^n(\eta_2')\chi_j^{m*}(\eta_2')\,\mathrm{d}\eta_2' = \delta_{mn}, \tag{2.34}$$

where

$$\phi_i^n(x_2) = \left[\delta^{-1/2}\right] \chi_i^n(\eta) \tag{2.35}$$

and

$$\Lambda_n(t) = \left[U_s^2 \delta\right] \tilde{\Lambda}_n. \tag{2.36}$$

The ratios, $Q_s^{i,j}/U_s^2$, are constants that would depend only on the growth-rate parameter, β. Thus, the motions can be represented in similarity variables in the inhomogeneous direction just as with the spectra in the homogeneous directions.

3. Comparison with data

It can only be determined by examining experiments whether actual flows evolve in a manner consistent with the similarity solutions outlined in § 2, and whether flows generated with different source conditions would or would not approach different solutions. The predictions of the similarity analysis are compared here with data from direct numerical simulations (DNS) of temporally evolving wakes computed by Moser & Rogers (1994) that had a Reynolds number based on the initial mass flux deficit of 2000. The first simulation was initiated using two independent realizations from a DNS of a turbulent flat-plate boundary layer (Spalart 1988) and thus, is analogous to the wake behind a flat plate with turbulent boundary layers. Moser & Rogers also performed two forced wake simulations where the streamwise and cross-stream velocity components of the two-dimensional modes (with $k_3 = 0$) in the initial conditions were amplified by a factor of 5 and 20, respectively, producing large-scale structures that persisted into the far field. Following the convention in Moser *et al.* (1998) the three simulations are referred to as the 'unforced', 'forced', and 'strongly forced' wake simulations. Moser *et al.* found that the 'unforced' wake simulation and the 'forced' wake simulation had extended periods during which the single-point moments evolved in an approximately self-similar manner. The third 'strongly forced' wake did not have an extended self-similar period, so this simulation is not considered here.

The profiles of the turbulence Reynolds stresses in the unforced and forced wake simulations were also approximately self-similar, though there was some variation from self-similarity in the profiles of $\overline{u_2^2}$, particularly for the forced wake simulation. Moser *et al.* also examined separately the contributions from the coherent two-dimensional motions in the spanwise direction (with $k_3 < 4k_1$) and the incoherent more three-dimensional motions (with $k_3 > 4k_1$). (This division is consistent with the two-point similarity theory outlined here.) They found that the profiles of the contribution from the incoherent motions (with approximately 80 % and 50 % of the total turbulent kinetic energy in the unforced and forced wakes, respectively) collapsed when they were plotted in similarity variables; the profiles for the contribution from the coherent motions did not. As noted in Moser *et al.*, McIlwain, Ewing & Pollard (1997) found most of the energy in these coherent motions was from motions with $k_3 = 0$ and the lowest wavenumbers in the streamwise direction. Thus, it was thought that the deviation from self-similar behaviour in the wake may be due to the effect of the finite size of the computational domain used in the simulations.

Data from four times during the self-similar period in each wake are examined here to determine whether measures of the two-point velocity correlation were evolving in a manner consistent with the equilibrium similarity solutions deduced in § 2. The one-dimensional spectra of the u_1 and u_2 components in the streamwise direction along the centreline of the 'unforced' and 'forced' wake at the different times are

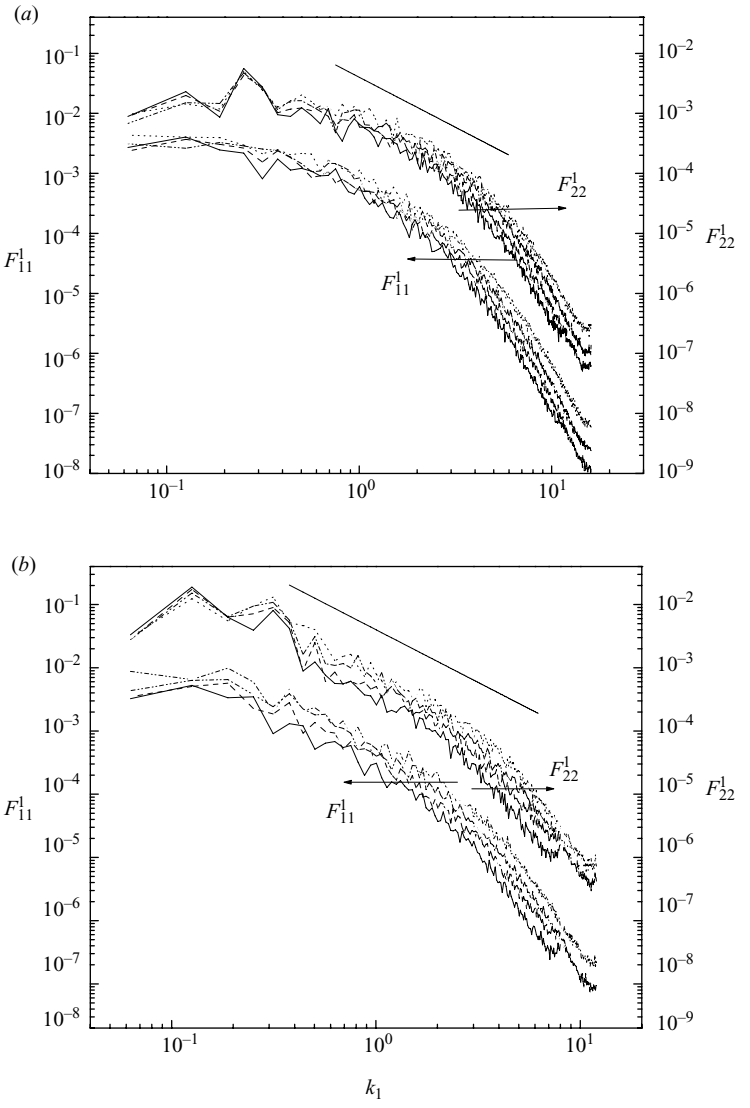

FIGURE 1. One-dimensional spectra, F_{11}^1 and F_{22}^1 at the centreline of the (*a*) unforced and (*b*) forced wake simulations at the times when δ/δ_o were ———, 3.594 and 5.306; – – –, 4.008 and 6.037; — – —, 4.446 and 6.636; and ·····, 4.884 and 7.235, respectively. The straight lines here are proportional to $k_1^{-5/3}$.

shown in figure 1. The spectra here have been averaged in the spatially homogeneous x_3-direction that was not transformed. There appear to be short ranges of $k_1^{-5/3}$ in the spectra from both wakes. These ranges are of greater extent in the forced wake because the turbulence Reynolds numbers of this flow is greater. The spectra from the forced wake also have a larger energy content in the low wavenumber region because of the organized structures present in this wake owing to the initial forcing. The spectra in both wakes decrease in magnitude and shift to lower wavenumbers as the wakes evolve, as predicted in the analysis.

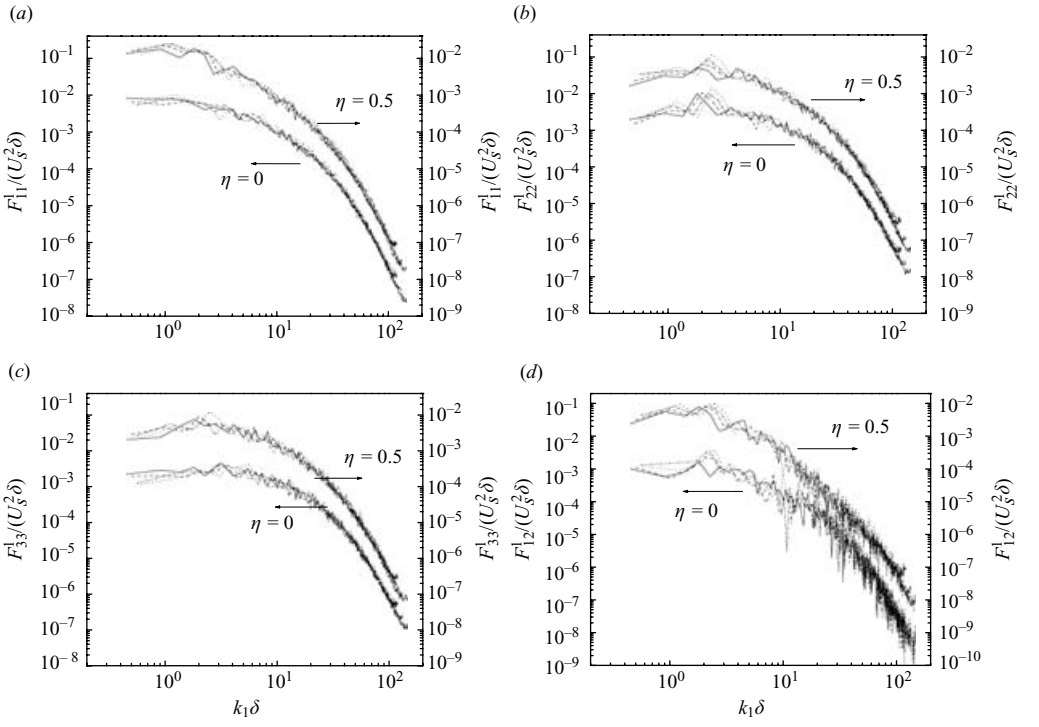

FIGURE 2. Scaled one-dimensional spectra, (*a*) $\tilde{F}_{11}^1$, (*b*) $\tilde{F}_{22}^1$, (*c*) $\tilde{F}_{33}^1$, and (*d*) $\tilde{F}_{12}^1$ at two cross-stream locations in the unforced wake when $\delta/\delta_o =$ ———, 3.594; – – –, 4.008; — — —, 4.446; and ·····, 4.884, respectively.

The one-dimensional spectra of the fluctuating velocity components and the cross-spectra in the streamwise and lateral directions of the unforced wake, scaled using similarity variables, are shown in figures 2 and 3. The one-dimensional spectra from the different times collapsed for most wavenumbers. There was some scatter at the highest wavenumbers caused by the change in the effective resolution of the computational grid as the small-scale motions grew in size, or by a change that was made during the simulation to a coarser grid once the small-scale motions were sufficiently large. There was also scatter at the lower wavenumbers, though much of this seems to be due to uncertainty in the computed spectra. In particular, the lengths of the computational domain in the lateral and streamwise directions are approximately 5 and 10 times the integral length scale, respectively. Thus, there are only approximately 2 to 5 independent measures of the large-scale motions in each direction resulting in an uncertainty in the spectra of 45–70 % (cf. George, Beuther & Lumley 1978). This is reflected more significantly in the cross-spectra than the scalar spectra, as expected. The uncertainty in these spectra are much larger than the uncertainty in the spectra presented in the previous experimental investigations of the two-point similarity (e.g. Gordeyev & Thomas 2000; Gamard *et al.* 2004). Here, though, unlike in those experimental investigations, essentially the full range of motions are resolved in the homogeneous directions, making it possible to examine whether the different scales of motion in the flow are evolving in a manner consistent with the similarity theory. In particular, Moser *et al.* (1998) found that the ratio of the energy in the coherent and incoherent motions (defined in the manner outlined

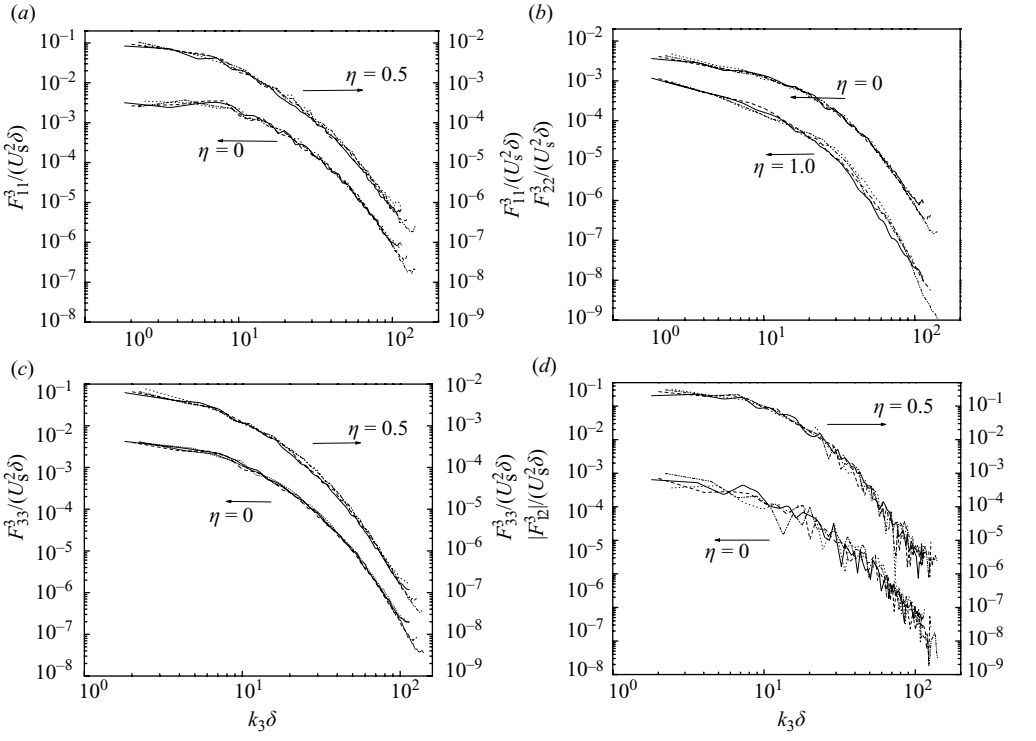

FIGURE 3. Scaled one-dimensional spectra, (*a*) $\tilde{F}_{11}^3$, (*b*) $\tilde{F}_{22}^3$, (*c*) $\tilde{F}_{33}^3$, and (*d*) $|\tilde{F}_{12}^3|$ at two cross-stream locations in the unforced wake when $\delta/\delta_o =$ ———, 3.594; – – –, 4.008; — – —, 4.446; and ·····, 4.884, respectively.

above) changed slowly over time in the unforced wake, indicating that these different motions were not evolving in complete equilibrium in this flow. The results here, though, show the spectra collapse surprisingly well, indicating that the turbulent motions in the unforced wake are evolving in a manner approximately consistent with the equilibrium similarity solutions deduced for the two-point equations.

The one-dimensional spectra of the fluctuating velocity and the cross-spectra in the streamwise direction of the forced wake, scaled using similarity variables, are shown in figure 4. The spectra collapse over a wide range of wavenumbers. There is more scatter in the low-wavenumber region of the streamwise spectra. Much of this again is likely statistical uncertainty in the computed spectra, but there seems to be a systemic change in the low-wavenumber range of F_{22}^1 that is not consistent with the similarity solutions, similar to the profiles of $\overline{u_2^2}$ in Moser *et al.* There is better collapse of the spectra in the x_3-direction, such as those shown in figure 5, in part, because much of the deviation from self-similar behaviour occurred in the two-dimensional modes with $k_3 = 0$, which are not shown in these spectra. The collapse of the spectra over most wavenumbers in both directions is a good indication that most of the motions in the forced wake are evolving in a manner consistent with the proposed equilibrium similarity solutions over the period considered here.

The results here, as in Moser *et al.*, suggest that the largest scales of motion in the forced wake simulation may not be evolving in a manner consistent with the equilibrium similarity solutions. This may be due to the finite computational domain size because the use of a computational domain (or experimental facility)

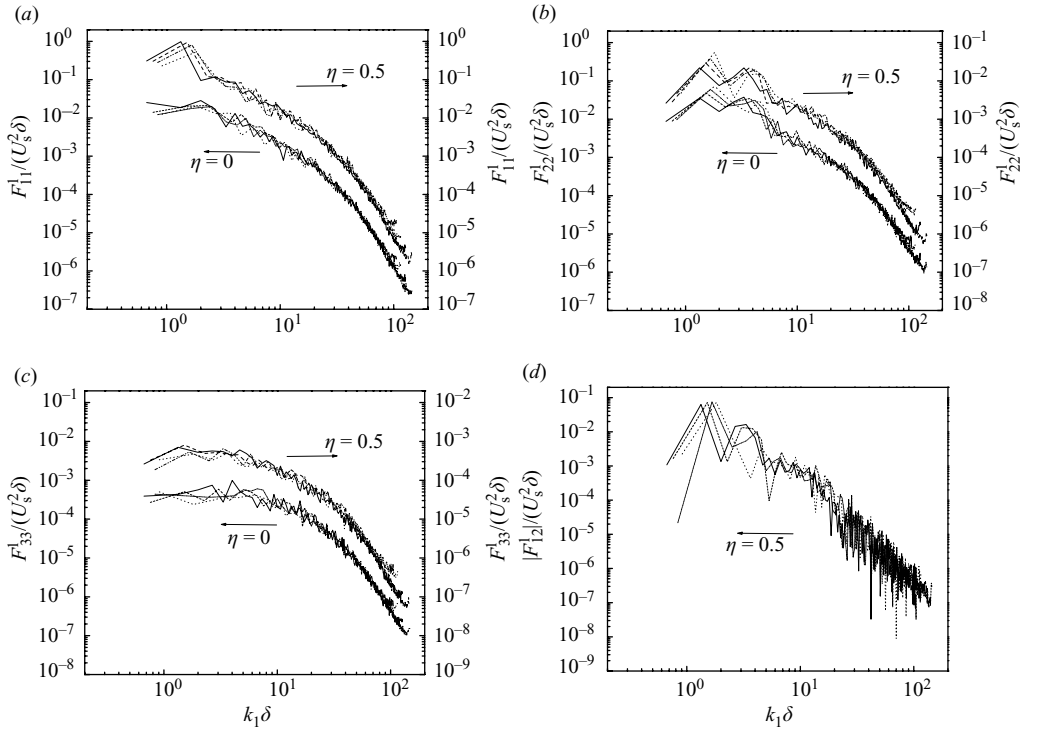

FIGURE 4. Scaled one-dimensional spectra, (*a*) $\tilde{F}^1_{11}$, (*b*) $\tilde{F}^1_{22}$, (*c*) $\tilde{F}^1_{33}$, and (*d*) $|\tilde{F}^1_{12}|$, at two cross-stream locations in the forced wake simulations when $\delta/\delta_o =$ ———, 5.306; – – –, 6.037; — – —, 6.636; and ·····, 7.235, respectively.

with finite lengths in the homogeneous directions imposes fixed length scales on the flow. At some point, these fixed length scales will conflict with the constraint from the similarity analysis that the length scales of the motions must grow continuously in all three directions as the flow evolves, resulting in deviation from self-similar behaviour. The constraints for the length scales in the homogeneous directions could not be deduced from the similarity analysis of the single-point equations. Thus, the similarity theory for the two-point velocity correlations may be useful in evaluating when the development of a flow is affected by the finite boundary conditions.

The correlations of the motions in the inhomogeneous direction were examined here using second-order structure functions given by (Monin & Yaglom 1975)

$$S^2_{\alpha\alpha}(r_1, x_2, x_2', r_3) = \overline{(u_\alpha - u_\alpha')^2}. \tag{3.1}$$

The structure function is relatively insensitive to the contribution from scales of motion larger than the separation distance between the points; thus it reduces the influence of the largest scales of motion that could be affected by the finite boundary conditions. The second-order structure functions for u_1 and u_2 computed at the centreline and the half-deficit points, $\eta = \pm 0.5$ in the unforced wake are shown in figure 6. The separation distances between the points in the streamwise and lateral directions, r_1 and r_3, were zero for these results. The similarity collapse of the structure functions is good for small separation distances ($\Delta\eta < 0.4$), but deteriorates for larger separations. The structure functions with larger separations are dominated by the large scales that are more affected by the limited statistical sample and that are more subject

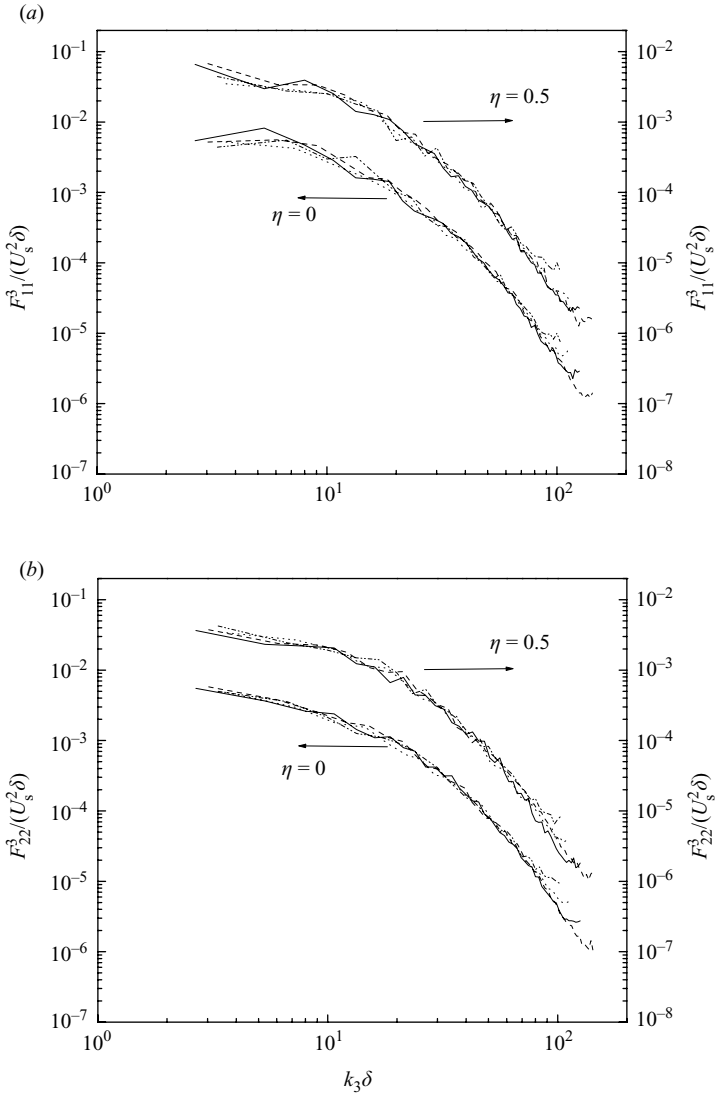

FIGURE 5. Scaled one-dimensional spectra, (*a*) $\tilde{F}_{11}^3$ and (*b*) $\tilde{F}_{22}^3$ at two cross-stream locations in the forced wake simulations when $\delta/\delta_o =$ ———, 5.306; – – –, 6.037; — — —, 6.636; and ·····, 7.235, respectively.

to finite domain size. The structure functions for the velocity components in the forced wake simulation did not collapse as well at large separation distances as those in the unforced wake, similar to the profiles of the single-point Reynolds stresses.

The similarity of the POD eigenvalues and eigenfunctions (predicted in § 2.1) was not directly tested using the DNS data because there were only approximately 10 independent measures in each DNS field, which is not sufficient for meaningful POD analysis. The noise apparent in the cross-spectra and structure functions is characteristic of this small sample. Further, unlike the Fourier decomposition, the eigenfunctions determined from the POD are sensitive to this noise, so the uncertainty in the eigenfunctions and eigenvalues are more difficult to characterize.

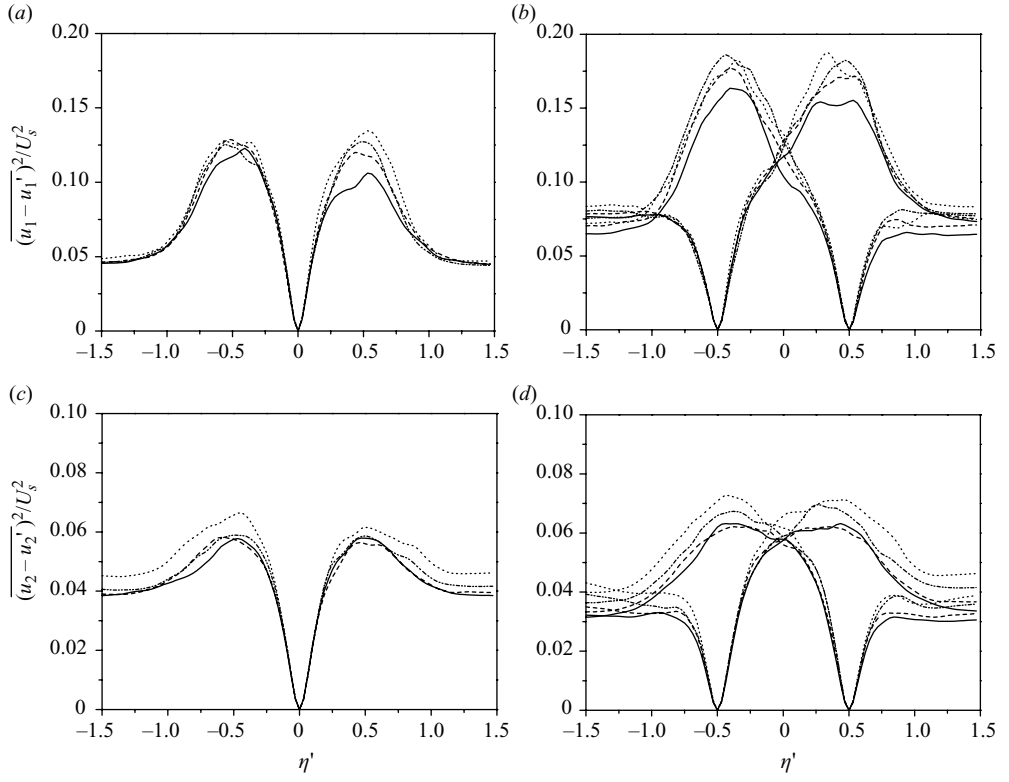

FIGURE 6. Scaled second-order structure function of the turbulent velocity field for (*a*) and (*b*) u_1 and (*c*) and (*d*) u_2 about the centreline in (*a*) and (*c*) and the half-deficit point ($\eta = \pm 0.5$) in (*b*) and (*d*) in the unforced wake when $\delta/\delta_o =$ ———, 3.594; – – –, 4.008; — - —, 4.446; and ·····, 4.884, respectively.

4. Further implications of the two-point similarity

In the similarity analysis of the single-point equations, it is assumed that the pressure–strain and the dissipation terms have equilibrium similarity solutions. These single-point moments are inherently two-point because the variation in the pressure is linked to the surrounding flow field and the dissipation depends on the local velocity gradient. Similarly, it is often assumed that the characteristic length scales of the turbulent motions can be scaled using a characteristic length of the flow in this constant-Reynolds-number flow when it is evolving in a equilibrium similarity manner. These results cannot be derived from the single-point solutions, but can be derived from the similarity solutions for the two-point velocity correlation tensor.

4.1. *Pressure–velocity correlations*

For example, the relationship between the two-point pressure velocity correlations and the two-point velocity correlations can be deduced from (e.g. Hinze 1975)

$$\frac{\partial^2 \overline{pu_j'}}{\partial x_k \partial x_k} = -2\frac{\partial U_k}{\partial x_l}\frac{\partial \overline{u_l u_j'}}{\partial x_k} - \frac{\partial^2 \overline{u_k u_l u_j'}}{\partial x_k \partial x_l}, \tag{4.1}$$

For a free shear flow such as the temporally evolving wake, this can be integrated to yield

$$\frac{\overline{pu'_j}}{\rho} = -\frac{1}{4\pi}\int 2\left[\frac{\partial U''_k}{\partial x''_l}\frac{\partial \overline{u''_l u'_j}}{\partial x''_k}\right]\frac{\mathrm{d}x''_1\mathrm{d}x''_2\mathrm{d}x''_3}{|x''_\alpha - x_\alpha|} - \frac{1}{4\pi}\int \frac{\partial^2 \overline{u''_k u''_l u'_j}}{\partial x''_k \partial x''_l}\frac{\mathrm{d}x''_1\mathrm{d}x''_2\mathrm{d}x''_3}{|x''_\alpha - x_\alpha|}, \tag{4.2}$$

where $|x''_\alpha - x_\alpha|$ is the magnitude of the distance between the point x''_α and x_α. Substituting the similarity solutions of § 2 into this equation yields

$$\begin{aligned}\frac{\overline{pu'_j}}{\rho} = {} & \frac{1}{2\pi}\left[U_s Q_s^{2,j}\right]\int \frac{\partial f(\eta'')}{\partial \eta''}\frac{\partial q_{2,j}(\zeta''+\zeta, \eta'', \eta', \xi''+\xi)}{\partial \zeta''} \\ & \times \frac{l_3 \mathrm{d}\zeta''\mathrm{d}\eta''\mathrm{d}\xi''}{\left[(l_1\zeta'')^2 + (\eta''-\eta)^2 + (l_3\xi'')^2\right]^{1/2}} - \frac{1}{4\pi}\left[T_{s,1}^{ki,j}\right]\int\left[\frac{\delta_{k1}}{l_1}\frac{\partial}{\partial\zeta''} + \delta_{k2}\frac{\partial}{\partial\eta''} + \frac{\delta_{k3}}{l_3}\frac{\partial}{\partial\xi''}\right] \\ & \times \left[\frac{\delta_{l1}}{l_1}\frac{\partial}{\partial\zeta''} + \delta_{l2}\frac{\partial}{\partial\eta''} + \frac{\delta_{l3}}{l_3}\frac{\partial}{\partial\xi''}\right] t^1_{kl,j}(\zeta''+\zeta, \eta'', \eta', \xi''+\xi) \\ & \times \frac{l_1 l_3 \mathrm{d}\zeta''\mathrm{d}\eta''\mathrm{d}\xi''}{\left[(l_1\zeta'')^2 + (\eta''-\eta)^2 + (l_3\xi'')^2\right]^{1/2}},\end{aligned} \tag{4.3}$$

where $\zeta'' = (x''_1 - x_1)/\delta_1$, $\xi'' = (x''_3 - x_3)/\delta_3$, and $\eta'' = x''_2/\delta$ are similarity variables, while $l_1 = \delta_1/\delta$ and $l_3 = \delta_3/\delta$ are the ratios of the length scales. Using the constraints for $T_{s,1}^{ki,j}$ and $Q_s^{2,j}$ from § 2, it is straightforward to show from the analysis here that the scale for the two-point pressure velocity correlation, $(\Pi_{s,1}^{i,j})$ must be proportional to $U_s^3(t)$, consistent with the constraint deduced in (2.26). This is not unexpected since the constraint that divergence of $\overline{pu'_j}$ must be zero was used in the analysis in § 2. The result illustrates, however, that the flow must be evolving in equilibrium with itself in order for there to be a 'local' equilibrium.

4.2. *Dissipation and the two-point vorticity correlation*

Similarly, the relationship between the two-point velocity gradient correlation and the two-point velocity correlation can be deduced by recognizing that (cf. Hinze 1975)

$$\overline{\frac{\partial u_i}{\partial x_k}\frac{\partial u'_j}{\partial x'_l}} = \frac{\partial^2}{\partial x_k \partial x'_l}(\overline{u_i u'_j}), \tag{4.4}$$

since u_i is not a function of x'_i nor u'_j a function of x_i. Substituting the proposed equilibrium solution for the two-point velocity correlation into this equation and transforming the derivatives, it follows that

$$\overline{\frac{\partial u_i}{\partial x_k}\frac{\partial u'_j}{\partial x'_l}} = \left[\frac{Q^{i,j}}{\delta^2}\right] h_{i,j;k,l}(\zeta, \eta, \eta', \xi, Re, *), \tag{4.5}$$

where $h_{i,j;k,l}$ is the resulting equilibrium similarity solution for the velocity derivative moments. As a result, the dissipation of the turbulent kinetic energy given by

$$\epsilon = \lim_{x_k \to x'_k} 2\nu\overline{s_{ij}s'_{ij}}, \tag{4.6}$$

where s_{ij} is the rate of strain from the fluctuating velocity field, has an equilibrium similarity solution that can be written in either the form for low-Reynolds-number

flows or for high-Reynolds-number flows; i.e.

$$\epsilon = \left[\frac{\nu U_s^2}{\delta^2}\right] d_L(\eta, Re, *) = \left[\frac{U_s^3}{\delta}\right] d_H(\eta, Re, *), \tag{4.7}$$

where

$$d_L(\eta, Re, *) = \frac{1}{Re_\delta} d_H(\eta, Re, *). \tag{4.8}$$

The most appropriate scale to collapse the dissipation profiles from different wakes will depend on the Reynolds number of the wakes.

It also follows that the two-point correlation of the vorticity has an equilibrium similarity solution of the form

$$\begin{aligned}\overline{\omega_i \omega_l'} &= \epsilon_{ijk}\epsilon_{lmn} \overline{\frac{\partial u_k}{\partial x_j}\frac{\partial u_n'}{\partial x_m'}} \\ &= \left[\frac{Q^{i,l}}{\delta^2}\right] v_{i,l}(\zeta, \eta, \eta', \xi, Re, *).\end{aligned} \tag{4.9}$$

(Note, that this is true, independent of any assumptions about local homogeneity, e.g. that $\overline{\omega_i \omega_i} = 2\nu \overline{s_{ij} s_{ij}}$.) Thus, all of the two-point statistical measurements of the structures in the temporally evolving wake should evolve in an equilibrium similarity manner, whether they are characterized using the velocity field or the vorticity field.

4.3. *Length scale and velocity scales*

The existence of two-point equilibrium similarity solutions in the temporally evolving wake implies that all of the dynamically relevant length scales in the flow should grow at the same rate. This can be shown for a number of length and velocity scales commonly used to characterize turbulent motions. For example, the integral length scales, used as measures of the energy-containing scales of motion (Monin & Yaglom 1975), can be written as

$$L_{\alpha\alpha}^1 = \frac{1}{\overline{u_\alpha^2}} \int_0^\infty \overline{u_\alpha(x_1, x_2, x_3, t) u_\alpha(x_1', x_2, x_3, t)}\, \mathrm{d}r_1 \tag{4.10}$$

$$= [\delta_1] \frac{1}{k_{\alpha\alpha}(\eta)} \int_0^\infty q_{\alpha,\alpha}(\zeta, \eta, \eta, 0)\, \mathrm{d}\zeta, \tag{4.11}$$

$$L_{\alpha\alpha}^2 = [\delta] \frac{1}{k_{\alpha\alpha}(\eta)} \int_{\eta'_{max}}^\infty q_{\alpha,\alpha}(0, \eta, \eta', 0)\, \mathrm{d}\eta', \tag{4.12}$$

$$L_{\alpha,\alpha}^3 = [\delta_3] \frac{1}{k_{\alpha\alpha}(\eta)} \int_0^\infty q_{\alpha,\alpha}(0, \eta, \eta, \xi)\, \mathrm{d}\xi, \tag{4.13}$$

where $k_{\alpha\alpha}(\eta)$ is the similarity solution for the single-point moment, $\overline{u_\alpha^2}$.

Similarly, the Taylor microscales, often thought of as the scale of the vorticity in the flow (Tennekes & Lumley 1972), given by

$$\lambda_{\alpha,\alpha}^\gamma(x_2) = \left[-2\overline{u_\alpha^2} \left(\frac{\partial^2 R_{\alpha,\alpha}}{\partial x_\gamma'^2}\bigg|_{x_\beta = x_\beta'} \right)^{-1}\right]^{1/2} \tag{4.14}$$

can be written as

$$\lambda^1_{\alpha,\alpha} = [\delta_1]\left[-2k_{\alpha\alpha}(\eta)\left(\left.\frac{\partial^2 q_{\alpha,\alpha}(\zeta,\eta,\eta,0)}{\partial\zeta^2}\right|_{\zeta=0}\right)^{-1}\right]^{1/2}, \tag{4.15}$$

$$\lambda^2_{\alpha,\alpha} = [\delta]\left[-2k_{\alpha\alpha}(\eta)\left(\left.\frac{\partial^2 q_{\alpha,\alpha}(0,\eta,\eta',0)}{\partial\eta'^2}\right|_{\eta=\eta'}\right)^{-1}\right]^{1/2}, \tag{4.16}$$

$$\lambda^3_{\alpha,\alpha} = [\delta_3]\left[-2k_{\alpha\alpha}(\eta)\left(\left.\frac{\partial^2 q_{\alpha,\alpha}(0,\eta,\eta,\xi)}{\partial\xi^2}\right|_{\xi=0}\right)^{-1}\right]^{1/2}. \tag{4.17}$$

Finally, the Kolmogorov length and velocity scales, which are measures of the smallest scales of motion, can be written as

$$\eta_k = \left(\frac{\nu^3}{\epsilon}\right)^{1/4} \propto \left(\frac{\nu^3\delta}{U_s^3}\right)^{1/4} = \frac{1}{Re_\delta^{3/4}}\delta, \tag{4.18}$$

$$u_k = (\epsilon\nu)^{1/4} \propto \left(\frac{U_s^3\nu}{\delta}\right)^{1/4} = \frac{1}{Re_\delta^{1/4}}U_s. \tag{4.19}$$

Thus, all of the length and velocity scales are proportional to the single-point length and velocity scales in the temporally evolving wake. As a result, measures of the small-scale motions will probably collapse when scaled with Kolmogorov variables, even for wakes with finite Reynolds numbers.

The Taylor microscale is often used to characterize the length scale of the turbulence in direct numerical simulations because it is the length scale that can be most accurately computed in these simulations. The change in the Taylor microscales computed from the u_1 components in the unforced and forced wake simulations, normalized by the similarity length scale, are shown in figure 7. The scaled Taylor microscales do not appear to remain constant as predicted in (4.15) and (4.17), particularly in the forced wake where the scaled microscales appear to decline as the wake thickens. The variation is relatively small in magnitude (approximately 15 % in the worst case), and there is significant statistical uncertainty in the Taylor microscale determined from the DNS fields, perhaps as high as 25 %. Thus, it is not possible to make a definitive statement regarding the scaling of the microscale in the DNS. If the trend in the scaled microscale is real, it may be an effect of finite domain size on the large scales. This would be consistent with the experience of Wang & George (2002) who found that the restrictions on the domain size in DNS of isotropic turbulence resulted in an under prediction of the Taylor microscales that worsened as the flow evolved and the length scale of the turbulence increased. This effect in the wake simulations would be more prevalent at the half-width where the large-scale motions reside.

5. Summary and concluding remarks

The governing equations for the two-point correlations of the turbulent fluctuating velocity in the temporally evolving wake were analysed and it was found that these equations admit equilibrium similarity solutions for finite-Reynolds-number wakes. The two-point velocity correlations could be written as a product of a time-dependent scale and a function dependent only on a single set of similarity variables.

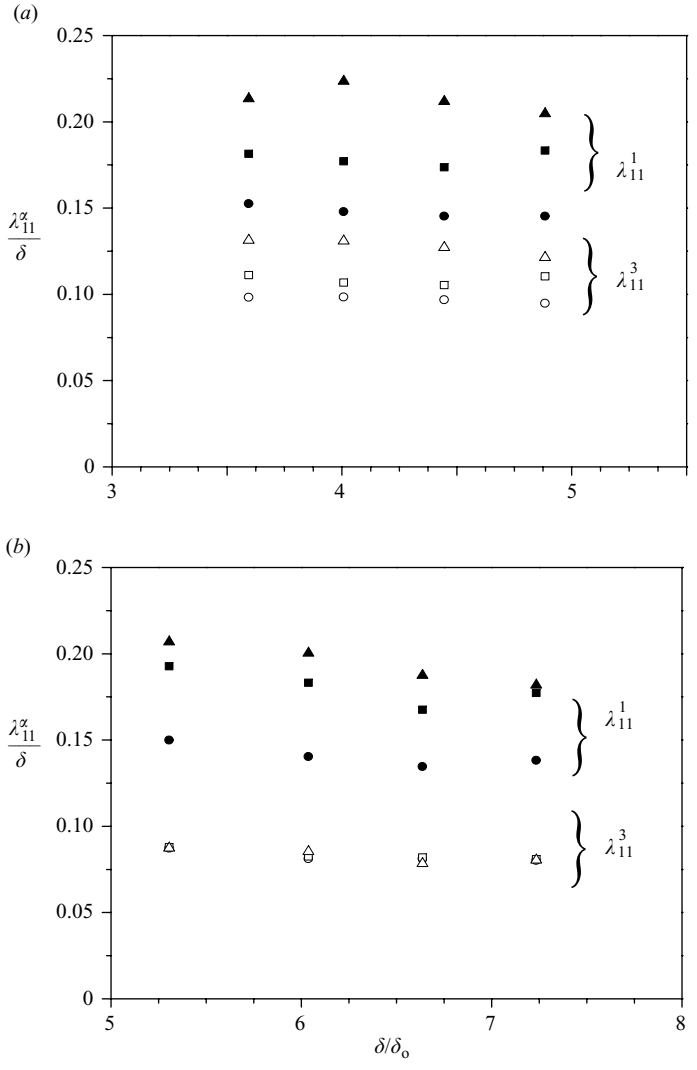

FIGURE 7. Change in the Taylor microscale determined from the spectra of u_1 in the (*a*) unforced and (*b*) forced wake at ○, $\eta = 0$; □, $\eta = 0.25$; and △, $\eta = 0.5$.

The equilibrium similarity solutions for the single-point equations in the temporally evolving wake given by Moser *et al.* (1998) are consistent with the similarity solutions for the two-point velocity correlation tensor deduced here. The similarity solutions for the two-point velocity correlations are more general, and they can be used to verify the scales for the pressure–strain terms and the dissipation terms in the single-point equations, which are inherently two-point quantities.

Physically, the production and dissipation of energy at the different scales of motion in the flow as well as the energy transfer between the different scales of motion are in equilibrium when the flow is evolving in a manner consistent with the proposed equilibrium similarity solutions. Since the local Reynolds number does not change as the flow evolves downstream, the characteristic length scales in all three directions and all of the dynamically important length scales in the flow are proportional. The one-dimensional Fourier spectra and the orthogonal functions and

eigenspectra deduced from the proper orthogonal decomposition could be written in an equilibrium similarity form when the two-point velocity correlation tensor has an equilibrium similarity solution.

Like the earlier single-point analysis, it was found that the governing equations for the equilibrium similarity solutions could not be reduced to a form that was independent of a growth-rate-dependent parameter. Thus, there is not a single 'universal' solution that describes the measures of the large-scale structures, and the large-scale structures at long times may depend on how the flow is generated. It was not possible to determine from the analysis whether wakes generated from different initial conditions would or would not approach different solutions, only that the equations allow for different similarity states. Experiments, however, show a clear dependence. As noted by George (1989) and in Moser *et al.* (1998), the differences in the similarity solutions for wakes do not appear in the mean velocity profiles or even in the properly scaled profiles of the Reynolds shear stress, but do appear in the growth rate and higher-order moments that incorporate more information about the underlying turbulent structures.

The predictions of the similarity analysis were compared to data from two direct numerical simulations of temporally evolving wakes examined by Moser *et al.* (1998). The one-dimensional spectra computed from these simulations collapsed reasonably well over the entire range of scales when they were scaled in the manner predicted by the equilibrium similarity analysis. The correlation in the inhomogeneous direction was examined using structure functions to reduce the effect of the largest scales of motion. These functions collapsed for most of the scales of motion in the flow over the time interval examined here. Thus, the equilibrium similarity solutions for the two-point correlation do seem to describe the evolution of the turbulent motions in the similarity region of the temporally evolving wake.

The periodic boundary conditions used in these simulations (or the finite facility size in experiments) impose fixed length scales on the problem that are not consistent with the equilibrium similarity solutions that require the length scales in all directions to grow as the flow evolves. At some point this affects the dynamics of the largest scales of motion and causes a deviation from the predictions of the equilibrium similarity analysis. Such a deviation from the equilibrium similarity solutions was observed here, and in the single-point profiles. Overall, though, the collapse of the data was good, indicating that most of the motions seem to evolve in a manner consistent with the equilibrium similarity solutions, even when the largest-scale motions are affected by the finite boundary conditions. The departures from equilibrium similarity may be a useful indicator of when the finite domain and periodic boundary conditions of the computations affect the solution.

The work here was part of the PhD dissertation of D. E. Earlier versions of some parts of the analysis and results have been presented in Ewing *et al.* (1995, 1996) and Ewing (2001). The work was supported in part by the Center for Turbulence Research at Stanford University and the National Science Foundation.

REFERENCES

Antonia, R. A., Browne, L. W. B., Bisset, D. K. & Fulachier, L. 1987 A description of the organized motion in the turbulent far wake of a cylinder at low Reynolds number. *J. Fluid Mech.* **184**, 423–444.

Batchelor, G. K. 1948 Energy decay and self-preserving correlation functions in isotropic turbulence. *Q. Appl. Maths* **6**, 97–116.

Bonnet, J. P., Delville, J. & Garem, H. 1986 Space and space-time longitudinal velocity correlations in the turbulent far wake of a flat plate in incompressible flow. *Exps. Fluids* **4**, 189–196.

Brede, M., Leder, A. & Westergaard, C. 2003 Time-resolved PIV investigation of the separated shear layer in the transitional cylinder wake. In *Proc. 5th Intl Symp. on Particle Image Velocimetry PIV 03* (ed. K. C. Kim), p. 3215. The Korean Society of Visualization, Pusan, Korea.

Durbin, P. A. & Reif, B. A. P. 2001 *Statistical Theory and Modeling for Turbulent Flows*. John Wiley.

Ewing, D. 1995 On multi-point similarity solutions in turbulent free-shear flows. PhD thesis, State University of New York at Buffalo.

Ewing, D. 2001 Evolution of the large-scale structures in the far-field of turbulent shear flows. In *Coherent Structures in Complex System* (ed. D. Regura, L. Bonilla & J. Rubi), Lecture Notes in Physics vol. 567, pp. 92–102. Springer.

Ewing, D. & George, W. K. 1995 Similarity analysis of the two-point velocity correlation tensor in a turbulent axisymmetric jet. In *Turbulence, Heat, and Mass Transfer I* (ed. K. Hanjalic & J. C. F. Pereira), pp. 49–56. Begell House.

Ewing, D. W., George, W. K., Moser, R. D. & Rogers, M. M. 1995 A similarity hypothesis for the two-point correlation tensor in a temporally evolving plane wake. In *Annual Research Brief 1995*, pp. 163–174. Stanford University: Center for Turbulence Research.

Ewing, D., George, W. K., Moser, R. D. & Rogers, M. M. 1996 A similarity hypothesis for the two-point velocity correlations in a temporally evolving wake. In *Advances in Turbulence VI* (ed. S. Gavrilakis, L. Machiels & P. Monkewitz), pp. 223–226. Kluwer.

Gamard, S., Jung, D. & George, W. K. 2004 Downstream evolution of the most energetic modes in a turbulent axisymmetric jet at high Reynolds number. Part 2. The far-field region. *J. Fluid Mech.* **514**, 205–230.

George, W. K. 1989 The self-preservation of turbulent flows and its relation to initial conditions and coherent structures. In *Advances in Turbulence* (ed. W. K. George & R. E. Arndt), pp. 39–73. Hemisphere.

George, W. K. 1992 The decay of homogeneous isotropic turbulence. *Phys. Fluids* A **4**, 1492–1507.

George, W. K. 1995 Some new ideas for similarity of turbulent shear flows. In *Turbulence, Heat, and Mass Transfer I* (ed. K. Hanjalic & J. C. F. Pereira), pp. 13–24. New York: Begell House.

George, W. K. & Gibson, M. M. 1992 The self preservation of homogeneous shear flow turbulence. *Exps. Fluids* **13**, 229–238.

George, W. K., Beuther, P. D. & Lumley, J. L. 1978 Processing of random signals. In *Proc. of the Dynamic Flow Conference, Skovlunde, Denmark*, pp. 757–800.

Ghosal, S. & Rogers, M. M. 1997 A numerical study of self-similarity in a turbulent plane wake using large-eddy simulation. *Phys. Fluids* **9**, 1729–1739.

Gordeyev, S. V. & Thomas, F. O. 2000 Coherent structure in the turbulent plane jet. Part 1. Extraction of proper orthogonal eigenmodes and their self-similarity. *J. Fluid Mech.* **414**, 145–194.

Grant, H. L. 1958 The large eddies of turbulent motion. *J. Fluid Mech.* **4**, 149–190.

Hayakawa, M. & Hussain, F. 1989 Three-dimensionality of organized structures in a plane turbulent wake. *J. Fluid Mech.* **206**, 375–404.

Hinze, J. O. 1975 *Turbulence*. McGraw-Hill.

Hussein, H. J., Capp, S. P. & George, W. K. 1994 Velocity measurements in a high-Reynolds-number, momentum-conserving, axisymmetric, turbulent jet. *J. Fluid Mech.* **258**, 31–75.

Johansson, P. B. V. & George, W. K. 2006 The far downstream evolution of the high Reynolds number axisymmetric wake behind a disk. Part 2. Slice proper orthogonal decomposition. *J. Fluid Mech.* **555**, 363–385.

Johansson, P. B. V., George, W. K. & Gourlay, M. J. 2003 Equilibrium similarity, effects of initial conditions and local Reynolds number on the axisymmetric wake. *Phys. Fluids* **15**, 603–617.

von Kármán, T. & Howarth, L. 1938 On the statistical theory of isotropic turbulence. *Proc. R. Soc. Lond.* (A) **164**, 476.

Keffer, J. F. 1965 The uniform distortion of a turbulent wake. *J. Fluid Mech.* **22**, 135–159.

Lumley, J. L. 1970 *Stochastic Tools*. Academic.

McIlwain, S., Ewing, D. & Pollard, A. 1997 Evolution of large- and small-scale coherent stuctures in non-homogeneous shear flows. *Bull. Am. Phys. Soc.* **41**, 1816.

Maekawa, H., Mansour, N. N. & Buell, J. C. 1992 Instability mode interactions in a spatially developing plane wake. *J. Fluid Mech.* **235**, 223–254.

Mi, J., Nobes, D. S. & Nathan, G. S. 2001 Influence of jet exit conditions on the passive scalar field of an axisymmetric free jet. *J. Fluid Mech.* **432**, 91–125.

Monin, A. S. & Yaglom, A. M. 1975 *Statistical Fluid Mechanics*, vol. 2. MIT Press.

Moser, R. D. & Rogers, M. M. 1994 Direct simulation of a self-similar plane wake. *Tech. Rep.* TM 108815. NASA Tech. Memo.

Moser, R. D., Rogers, M. M. & Ewing, D. 1998 Self-similarity of time-evolving plane wakes. *J. Fluid Mech.* **367**, 255–289.

Mumford, J. C. 1983 The structure of the large eddies in fully developed turbulent shear flows. Part 2. The plane wake. *J. Fluid Mech.* **137**, 447–456.

Narasimha, R. 1992 The utilities and drawbacks of traditional approaches. In *Whither Turbulence? Turbulence at the Crossroads* (ed. J. L. Lumley), pp. 13–49. Springer.

Pope, S. 2000 *Turbulent Flows*. Cambridge University Press.

Slessor, M. D., Bond, C. L. & Dimotakis, P. E. 1998 Turbulent shear-layer mixing at high Reynolds numbers: effects of initial conditions. *J. Fluid Mech.* **376**, 115–138.

Spalart, P. R. 1988 Direct simulation of a turbulent boundary layer up to $R_\theta = 1410$. *J. Fluid Mech.* **187**, 61–98.

Speziale, C. G. & Bernard, P. S. 1992 The energy decay in self-preserving isotropic turbulence revisited. *J. Fluid Mech.* **241**, 645–667.

Tennekes, H. & Lumley, J. L. 1972 *A First Course in Turbulence*. MIT Press.

Townsend, A. A. 1956 *The Structure of Turbulent Shear Flow*. Cambridge University Press.

Townsend, A. A. 1979 Flow patterns of large eddies in a wake and in a boundary layer. *J. Fluid Mech.* **95**, 515–537.

Wang, H. & George, W. K. 2002 The integral scale in homogeneous isotropic turbulence. *J. Fluid Mech.* **459**, 429–443.

Weygandt, J. H. & Mehta, R. D. 1993 Three-dimensional structure of straight and curved plane wakes. *Tech. Rep.* JIAA TR-110. Stanford University.

Williamson, C. H. K. & Prasas, A. 1993 A new mechanism for oblique wave resonance in the 'natural' far wake. *J. Fluid Mech.* **256**, 269–313.

Wygnanski, I., Champagne, F. & Marasli, B. 1986 On the large-scale structures in two-dimensional small-deficit, turbulent wakes. *J. Fluid Mech.* **168**, 31–71.